

Barrier penetration and spontaneous fission in the time-dependent mean-field approximation

S. Levit, J. W. Negele, and Z. Paltiel*

Center for Theoretical Physics, Laboratory for Nuclear Science and Department of Physics, Massachusetts Institute of Technology, Cambridge, Massachusetts 02139

(Received 20 May 1980)

A mean-field theory is obtained for the spontaneous decay of unstable nuclei by applying the stationary-phase approximation to a functional integral expression for $\text{Tr}(H - E)^{-1}$. The method is applied first to the lifetime of a metastable state in one-dimensional quantum mechanics and subsequently generalized to many-fermion systems. Solutions to the resulting nonlinear self-consistent field equations are presented for a self-bound, saturating many-body system of fermions in one spatial dimension.

NUCLEAR REACTIONS, FISSION Derivation of dynamical mean-field equations for spontaneous fission, using imaginary time stationary-phase approximation to a functional integral expression for $\text{Tr}(H - E)^{-1}$. Application to a many-fermion model in one spatial dimension.

I. INTRODUCTION

The objective of this work is to obtain a microscopic understanding of tunneling and spontaneous decay in terms of a quantum mean field theory comparable to that which has been achieved for nuclear ground states, collective and single-particle excited states, and the nuclear response function. Existing theories of fission, such as the generator coordinate theory¹ or the adiabatic time-dependent Hartree-Fock approximation² have the serious conceptual deficiency of requiring *ab initio* selection of specific degrees of freedom to be used as collective coordinates. Less microscopic formulations require, in addition, prescriptions for inertial parameters to be associated with the collective variables. In contrast, mean-field theories of deformed intrinsic states or nuclear collective motion allow all relevant degrees of freedom to enter self-consistently into the calculation of quantum observables without any artificial imposition of collective variables. Thus, we believe it is extremely desirable to develop a mean-field theory of tunneling in which the shape degrees of freedom and dynamics are specified solely in terms of the nuclear interaction.

The variational derivation of the time-dependent Hartree-Fock (TDHF) initial-value problem yields no insight into how the TDHF equations can be used to describe the spontaneous fission of a nucleus. Naive TDHF evolution starting from a static HF wave function is clearly inadequate, since the one-body density matrix remains time-independent. Moreover, the static HF solution for a fissile nucleus such as ²³⁸U is perfectly stable against small oscillations, although the state has higher energy than the energies of the fission fragments. The

situation is typical of the semiclassical approximation for tunneling decay and the decisive step in making the description of fission possible is to allow for the mean-field propagation in *imaginary time*. The solutions thus obtained are similar to instantons in relativistic field theories.³ Using a functional integral representation for the nuclear time evolution operator,⁴ we are able to extend these ideas to the description of tunneling in nuclear many-fermion problems.

The starting point for our formal development, as in our previous treatment of large amplitude collective motion,⁵ is a functional integral representation for

$$\text{Tr}(E - H + i\epsilon)^{-1} = -i \int_0^\infty dT e^{i(E+i\epsilon)T} \text{Tr} e^{-iHT}. \quad (1.1)$$

Using the stationary-phase approximation, we investigate the mean-field theory arising from the complex stationary points in the time integral appearing in Eq. (1).

Whereas it is possible to obtain precisely the same mean-field equations and penetrability through arguments analogous to Coleman's treatment³ of the decay of the false vacuum⁶ by evaluating the long time behavior of e^{-HT} , we believe the alternative derivation presented here offers specific advantages. Stationary solutions with complex time arise completely naturally through the application of the saddle-point method to the integral in Eq. (1). Furthermore, we avoid certain technical difficulties associated with evaluation of the determinant of the second functional derivative of the action in more than one dimension.

Thus, in Sec. II, we will show how to derive the decay rate in one-dimensional quantum mechanics

from summing a sequence of stationary contributions to Eq. (1) at well-separated points in the complex T plane. Subsequently, the method will be generalized to the many-body problem in Sec. III to determine a decay rate which is the sum over partial widths for decay into open breakup channels. As in the case of the static Hartree problem, to which the resulting theory has great structural similarity, little can be proven mathematically about the existence and properties of solutions to the coupled nonlinear integrodifferential equations derived in Sec. III. Therefore, in Sec. IV the theory is applied to a nontrivial model many-body system embodying many of the essential features of finite nuclei. Fermions with one spatial degree of freedom interacting through attractive short-range two-body forces are made to saturate by the introduction of a Skyrme-like repulsive three-body force, and to fission by including a long-range repulsive interaction analogous to the Coulomb interaction in three dimensions. Two-dimensional numerical tunneling solutions in time, and one spatial dimension are presented which explicitly display the structure assumed in the general treatment of Sec. III.

Finally, our conclusions, remaining open problems, and the prospects for application to nuclear fission in three spatial dimensions are discussed in the last section.

II. TUNNELING IN ONE DEGREE OF FREEDOM

The widths of unstable quantum mechanical states are conveniently determined by the complex poles of the energy-dependent propagator $(H - E)^{-1}$. We start in this section by considering an example of a problem with one degree of freedom q which is described by the Hamiltonian

$$H(p, q) = \frac{p^2}{2m} + V(q) \quad (2.1)$$

with a potential of the form shown by the solid line in Fig. 1. This problem obviously has unstable states in the region of energies $E_0 \leq E \leq E_b$, and we want to show how the stationary-phase approximation (SPA) to a functional integral which describes the motion should be applied in order to derive the widths of these states. Although the results of this simple example will not be new and could be obtained by other methods, the treatment which we present has the merit of being appropriate for a generalization to the many-nucleon case discussed in the next section.

For the problem defined by Eq. (2.1), we consider

$$\text{Tr}(H - E)^{-1} = -i \int_0^\infty dT e^{iET} \int dq \langle q | e^{-iHT} | q \rangle, \quad (2.2)$$

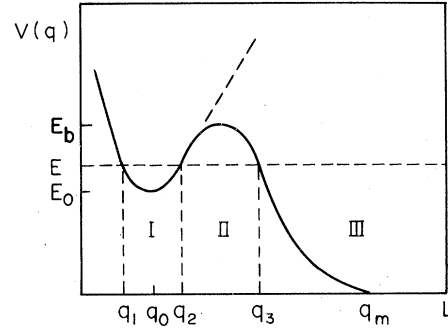


FIG. 1. Schematic diagram of potential having quasi-stable states. The relative minimum of the potential occurs at energy E_0 and coordinate q_0 , and the intercepts of an energy $E > E_0$ are denoted by q_1 , q_2 , and q_3 .

where E has a small positive imaginary part and $\text{Tr} \exp(-iHT)$ is calculated in coordinate representation. Using Feynman functional integral representation for the propagator,⁷ we write

$$\langle q | e^{-iHT} | q \rangle = \int Dq(t) e^{iS[q(t)]}, \quad (2.3)$$

where $S[q(t)]$ is the classical action calculated along an arbitrary trajectory $q(t)$ which satisfies the boundary conditions

$$q(0) = q(T) = q. \quad (2.4)$$

The integral in (2.3) is over all such $q(t)$, and $Dq(t)$ is a properly defined measure for this functional integration.⁷

The SPA for the integral in (2.3) results in

$$\langle q | e^{-iHT} | q \rangle \cong A e^{iS[q_{cl}(t)]}, \quad (2.5)$$

where $q_{cl}(t)$ is a solution of the classical equation

$$\delta S = 0, \quad (2.6)$$

subject to the boundary conditions (2.4). The amplitude A in (2.5) is associated with the small quadratic corrections around $q_{cl}(t)$.⁷ We will not need its explicit expression.

Using Eq. (2.5) in Eq. (2.2), we again evaluate the remaining integrals over q and T by SPA. The action $S[q_{cl}(t)]$ depends on q via the end points of the classical trajectory q_{cl} , Eq. (2.4). Therefore the SPA condition requires

$$0 = \frac{\partial S_{cl}}{\partial q} = \frac{\partial S_{cl}}{\partial q(0)} + \frac{\partial S_{cl}}{\partial q(T)} = -p_{cl}(0) + p_{cl}(T), \quad (2.7)$$

which together with (2.4) implies that only periodic classical trajectories satisfying

$$q_{cl}(0) = q_{cl}(T) \quad (2.8)$$

and

$$p_{cl}(0) = p_{cl}(T)$$

contribute to $\text{Tr} \exp(-iHT)$ in the SPA limit.

For the integral over T in (2.2), the SPA condition is

$$E = -\frac{\partial S_{cl}}{\partial T} \equiv E_{cl}(T). \quad (2.9)$$

Thus, the period of the classical trajectory should be such that the corresponding classical energy is equal to the value of E which appears in the left hand side of Eq. (2.2). The contribution to $\text{Tr}(H - E)^{-1}$ of a given solution T_{cl} of the condition (2.9) consists of a phase factor $e^{iW(E)}$ with

$$W(E) = ET_{cl} + S_{cl}(T_{cl}) \quad (2.10)$$

and a multiplicative amplitude similar to A in (2.5). The SPA result is obtained by the summation over *all* solutions T_{cl} of (2.9). In the energy range $E_0 \leq E \leq E_b$, one possible class of such solutions is generated by a classical trajectory traversing the classically allowed region I, $q_1 \leq q \leq q_2$, shown in Fig. 1. The period T_{cl} of this trajectory and the corresponding action W_1 are obviously given by integer multiples of the basic period

$$T_1(E) = 2 \int_{q_1}^{q_2} \left\{ \frac{m}{2[E - V(q)]} \right\}^{1/2} dq \quad (2.11)$$

and the basic action

$$W_1(E) = 2 \int_{q_1}^{q_2} \{2m[E - V(q)]\}^{1/2} dq. \quad (2.12)$$

For a potential with stable bound states, denoted by the dashed line in Fig. 1, this is the only possible class of solutions. In this case, the SPA approximation to the time integral in Eq. (2.2) thus yields an infinite sequence of stationary points along the real axis. Summation over all these stationary points yields the geometric series

$$\sum_{k=1}^{\infty} e^{ikhW_1(E)} = \frac{e^{iW_1(E)}}{1 - e^{iW_1(E)}} \quad (2.13)$$

with poles at energies defined by the quantization condition

$$W_1(E) \equiv 2 \int_{q_1}^{q_2} \{2m[E - V(q)]\}^{1/2} dq = 2N\pi, \quad N - \text{integer}. \quad (2.14)$$

This result differs from the familiar WKB quantization condition only because our neglect thus far of quadratic corrections has omitted the turning point phases required to obtain the proper factor $2(N + \frac{1}{2})\pi$. Precisely this type of SPA summation [Eq. (2.13)] was used in Ref. 5 to obtain quantized states of large amplitude nuclear collective motion.

In a potential with unstable bound states, two additional classes of classical solutions are pres-

ent. If one assumes, for simplicity, a large normalization box with infinite repulsive potential at $q=L$, classically allowed periodic solutions exist in region III, $q_3 < q < L$, completely analogous to those in region I, with action

$$W_3(E) = 2 \int_{q_3}^L \{2m[E - V(q)]\}^{1/2} dq \quad (2.15)$$

and period

$$T_3(E) = 2 \int_{q_3}^L \left\{ \frac{m}{2[E - V(q)]} \right\}^{1/2} dq. \quad (2.16)$$

In addition, a completely different class of classical solutions exists which correspond to traversing the classically forbidden region II, $q_2 \leq q \leq q_3$. Since in this region $E \leq V(q)$, the corresponding period

$$T_2(E) = 2 \int_{q_2}^{q_3} \left\{ \frac{m}{2[E - V(q)]} \right\}^{1/2} dq \quad (2.17)$$

is imaginary. The most general classical solution is obtained if one considers all possible trajectories in the two allowed and one forbidden regions. The stationary points in the complex T plane now constitute a lattice

$$T_{knl} = kT_1(E) + nT_2(E) + lT_3(E), \quad (2.18)$$

where k , n , and l are arbitrary positive integers, and the corresponding stationary phase contributions is

$$\exp[ikW_1(E) - nW_2(E) + ilW_3(E)], \quad (2.19)$$

where

$$W_2(E) = 2 \int_{q_2}^{q_3} \{2m[V(q) - E]\}^{1/2} dq. \quad (2.20)$$

Retaining the complex solutions of Eq. (2.9) is consistent with the general saddle point method in which all the stationary points of the integrand must be considered irrespective of whether or not they lie on the integration contour. The contour should then be deformed to pass through all the points in the direction of the steepest descent, and if these are far enough apart, the SPA result is given by the sum of the contributions from all these stationary points. Although a mathematically precise treatment of the SPA is beyond the scope of the present work, a relevant discussion of possible complications is found in Ref. 8.

To emphasize the essential physics of the decay width, let us first sum over the classical trajectories which involve all combinations of cycles in regions I and II. The trace over q is then approximated by the sum of all trajectories which begin and end in region I plus the sum of all those beginning and ending in region II. The first sum is conveniently performed by noting that any number

of cycles in region II may be attached to each cycle in region I, with the result

$$\sum_{k=1}^{\infty} \left[e^{iW_1} \left(\sum_{n=0}^{\infty} e^{-nW_2} \right) \right]^k = [1 - e^{iW_1}(1 - e^{-W_2})^{-1}]^{-1} - 1 = \frac{e^{iW_1}}{1 - e^{iW_1} - e^{-W_2}}. \quad (2.21)$$

We have omitted the quadratic correction factors analogous to the amplitude A in Eq. (2.5) and will discuss their role at the end of this section.

The corresponding sum for cycles beginning and ending in region II is obtained by interchanging iW_1 and $-W_2$, so that the final result is

$$\frac{e^{iW_1} + e^{-W_2}}{1 - e^{iW_1} - e^{-W_2}}, \quad (2.22)$$

which has poles at energies which satisfy

$$e^{iW_1(E)} + e^{-W_2(E)} = 1. \quad (2.23)$$

Assuming that $e^{-W_2(E)}$ is small, we may solve Eq. (2.23) iteratively. In zeroth approximation, we neglect $e^{-W_2(E)}$, in which case Eq. (2.23) reproduces the same WKB energies inside the well given by Eq. (2.14). Proceeding to the next iteration of Eq. (2.23), we denote by E_N the solution of Eq. (2.14) with given N , set $E = E_N + \Delta E_N$ in the first term of Eq. (2.23) and $E = E_N$ in the smaller second term. Expanding in powers of ΔE_N , one finds

$$\exp i \left[W_1(E_N) + \frac{\partial W_1(E_N)}{\partial E} \Delta E_N \right] + e^{-W_2(E_N)} = 1 \quad (2.24)$$

so that

$$\Delta E_N = \frac{1}{2} i \Gamma_N, \quad (2.25)$$

where

$$\Gamma_N = 2 \left[\frac{\partial W_1(E_N)}{\partial E} \right]^{-1} e^{-W_2(E_N)} = \frac{\omega_{c1}(E_N)}{\pi} e^{-W_2(E_N)}, \quad (2.26)$$

and we have used Eqs. (2.11) and (2.12) to rewrite $\partial W_1/\partial E$ in terms of the frequency $\omega_{c1}(E_N)$ of the allowed classical motion at $E = E_N$. This result of summing all cycles involving regions I and II thus reproduces the familiar WKB expression for the width of an unstable state in the limit of large W_2 , but with π instead of 2π in the denominator. This "missing" factor of $\frac{1}{2}$ is discussed in detail in Ref. 9 and the discussion is presumably also applicable in our case.

Although it is intuitively evident that trajectories in regions I and II should dominate the decay rate, it is still desirable to formally demonstrate that periodic solutions in region III do not contribute in the present order of approximation. Indeed, the sum over trajectories in regions I and II is conceptually incomplete, since we have not yet

had to specify whether we are working in a very small box, which would necessarily have well-separated real eigenvalues, or dealing with the physically interesting case of the limit of an arbitrarily large normalization box, for which the density of states approaches a continuum. A particularly convenient way of demonstrating that periodic trajectories in region III contribute negligibly to the physical decay rate is to calculate the smoothed density of states in an arbitrarily large normalization box, and this derivation is presented in Appendix A.

In conclusion, we observe that the decay width of an unstable state arises in the SPA as a result of the interference of the contributions from classical trajectories in classically allowed and forbidden regions I and II. The latter trajectories formally represent solutions of the classical equations in imaginary time [Eq. (2.17)]. The substitution $t = i\tau$ in the classical equation

$$\frac{d^2q}{dt^2} = -\frac{1}{m} \frac{\partial V}{\partial q}$$

is equivalent to reversing the sign of the potential V (see Fig. 1), thereby making the motion possible in the region which was classically inaccessible in the original problem.

It is important to emphasize that in the present context, the concept of imaginary time is a direct consequence of the stationary-phase evaluation of the time integral in Eq. (2.2) and effectively accounts for the quantum superposition of different real time intervals which contribute to the propagation with a given energy E in (2.2). It is also seen that when treated carefully, the SPA is rich enough to retain the part of the interference which approximately reproduces the correct resonance structure of $\text{Tr}(H - E)^{-1}$.

It is obvious that the value E_0 denoted in Fig. 1 satisfies the quantization condition (2.14) with $N = 0$. In this case, $\omega_{c1}(E_0)$ represents the frequency of the harmonic motion in the infinitesimal vicinity of $q = q_0$. The corresponding trajectory in the forbidden region has a part near q_0 where the motion is infinitely slow and the corresponding period $T_2(E_0)$ is infinitely large. Following Coleman,⁹ we call this trajectory a bounce.

Finally, we comment on the quadratic correction factors omitted in (2.13). It is known¹⁰ that their absolute values depend on the initial and final momenta $p(0)$ and $p(T)$ of a corresponding classical trajectory, analogous to the similar factors $p^{-1/2}$ in a WKB wave function. Since the trajectories included in (2.13) all have the same $p(0) = p(T)$, the absolute values of the quadratic corrections do not effect the poles of (2.13). Their phases are related to the turning points along a given trajectory

and will modify Eq. (2.13). Each of the turning points in the classically allowed region contributes $\pi/2$ so that $W_1(E)$ is replaced by $W_1(E) + \pi$. The right hand side of (2.14) will accordingly be changed to $(2M+1)\pi$. For the lowest state in the well, for instance, this will introduce the zero-point motion correction to the bottom of the well energy E_0 .

III. MEAN-FIELD EQUATIONS FOR SPONTANEOUS FISSION

As was presented in Ref. 4, the time-dependent mean-field approximation to the nuclear many-body evolution operator $U(T) = e^{-iHT}$ is conveniently discussed in the framework of the stationary-phase evaluation of a functional integral representing $U(T)$. Studying the poles of the energy transform of $U(T)$, it was shown in Ref. 5 how the SPA leads to periodic time-dependent mean-field solutions describing nuclear bound states. The particular case of a static solution reduces to the usual static HF approximation. In the situation where a nucleus can undergo spontaneous fission, the energetics of the problem obviously are such that along with the static HF solution describing the ground state of the fissioning nucleus, there exist time-dependent mean-field solutions with the same energy, corresponding to the asymptotic motion of fission fragments in all the open decay channels. These are simply the ground or excited states of the fragments boosted with the appropriate momentum to match the energy of the fissioning nucleus.

Since, as was discussed in the Introduction, the ordinary TDHF equations cannot, in principle, describe the tunneling process which connects these two solutions, we will now extend the SPA treatment of tunneling in one-dimensional quantum mechanics to the many-body problem by considering the mean-field approximation to $\text{Tr}e^{-iHT}$ for a general complex value of T . The counterpart of closed periodic classical trajectories will be periodic determinantal solutions to TDHF equations in real or imaginary time, so that the single degree of freedom q is replaced by the infinite number of degrees of freedom in the one-body density matrix of Slater determinants. Figure 1 is now replaced by a complicated multidimensional surface of classically allowed and forbidden regions, and we wish to explore all the stationary determinantal trajectories in this surface relevant to spontaneous decay of an unstable nucleus.

One immediate complication is the problem of connecting periodic solutions in allowed and forbidden regions. In Fig. 1, it is obvious that a trajectory which makes one cycle in region I followed

by a cycle in region II can be built up from a fundamental periodic solution in region I and a periodic solution in region II. However, in general, for the many-body problem, there is no assurance that a periodic determinantal wave function in a classically allowed region exactly equals that in a classically forbidden region at the turning point. Thus, the simplification in one dimension of summing a geometric series to build all trajectories out of a few fundamental solutions is, in general, replaced by the formidable task of constructing each multicycle trajectory independently. The case of spontaneous decay from an HF stationary state, however, is special in that a certain class of imaginary time tunneling solutions in the counterpart of region II do, in fact, join to the quasi-stable solution in region I. Thus, we will assume for the moment that such joining is possible and derive the equations of motion and corresponding contributions to the action for such periodic trajectories. It is, of course, crucial to the present development that we do not need to include contributions from the counterpart of region III, since at the outer turning point we are unable to join periodic solutions.

Applying the method of Ref. 4, we find it useful to start by defining a dimensionless parameter η such that

$$t = T\eta, \quad -\frac{1}{2} \leq \eta \leq \frac{1}{2}, \quad (3.1)$$

where t is the time variable and a symmetric interval is chosen for later convenience. The interaction representation of $U(T) = e^{-iHT}$ is expressed via density operators $\hat{\rho}(x)$ as

$$U(T) = T_\eta \exp \left[-iT \int_{-1/2}^{1/2} d\eta \times \int dx dx' \hat{\rho}(x, \eta) V(x-x') \hat{\rho}(x', \eta) \right], \quad (3.2)$$

where T_η denotes the ordering with respect to the parameter η ,

$$\hat{\rho}(x, \eta) = e^{iK'T\eta} \hat{\rho}(x) e^{-iK'T\eta}, \quad (3.3)$$

$$K' = K - \frac{A}{2} V(0),$$

K is the kinetic energy, V is the two-body interaction (taken for simplicity, spin-isospin independent), and A is the number of nucleons. In (3.2), a local form of the density operator was chosen to represent $U(T)$. As was discussed in Ref. 4, this will eventually lead to the Hartree rather than Hartree-Fock expressions for the mean field in the subsequent stationary-phase approximations. The way to obtain the full HF treatment was outlined in Ref. 5 (cf. also Ref. 11). We will not repeat it here

but for the sake of notational clarity will proceed on the basis of (3.2) and the Hartree approximation.

As in Ref. 4, we use the Hubbard-Stratonovich transformation to linearize the exponential (3.2) and obtain

$$U(T) = \int D\sigma e^{i(T/2)(\sigma, V\sigma)} U_\sigma(T), \quad (3.4)$$

where

$$U_\sigma(T) = T_\eta e^{-iT(\rho, V\sigma)}. \quad (3.5)$$

For notational convenience, we define

$$(\sigma, V\sigma) = \int_{-1/2}^{1/2} d\eta \int dx dx' \sigma(x, \eta) V(x-x') \sigma(x', \eta) \quad (3.6)$$

and similarly for $(\rho, V\rho)$.

Using Eq. (3.4), one obtains

$$\text{Tr}U(T) = \int D\sigma e^{i(T/2)(\sigma, V\sigma)} \text{Tr}U_\sigma(T). \quad (3.7)$$

To construct $\text{Tr}U_\sigma(T)$, we use the same procedure as in Ref. 5.

Consider a single particle equation

$$\left[i \frac{\partial}{\partial \eta} - T \left(\frac{p^2}{2m} - \frac{1}{2} V(0) + \int V(x-x') \sigma(x', \eta) dx' \right) \right] \phi_k = 0 \quad (3.8a)$$

with boundary conditions

$$\phi_k(x, \eta = \frac{1}{2}) = e^{-i\alpha_k} \phi_k(x, \eta = -\frac{1}{2}). \quad (3.8b)$$

Using the basis of states formed by the solutions of (3.8) with a given $\sigma(x, \eta)$ one obtains

$$\text{Tr}U_\sigma = \sum_{\{n_k\}} \exp -i \sum_{k=1}^{\infty} n_k \alpha_k[\sigma], \quad (3.9a)$$

where

$$n_k = 0 \text{ or } 1, \quad \sum_{k=1}^{\infty} n_k = A. \quad (3.9b)$$

The expression (3.9) holds, since Slater determinants built of single particle wave functions satisfying (3.8) are eigenfunctions of $U(T)$. The sum in (3.9) is over all possible sets of occupation numbers $\{n_k\}$ satisfying (3.9b). Notice that since T in (3.8) is allowed to be complex, the eigenvalues α_k are, in general, not real.

The stationary-phase condition for the integral over σ in (3.7) applied to each term in the sum (3.9a) separately reads

$$T \int V(x-x') \sigma(x', \eta) dx' = \sum_{k=1}^{\infty} n_k \frac{\delta \alpha_k}{\delta \sigma(x, \eta)}. \quad (3.10)$$

To calculate the right hand side of this expression, we write (3.8) in eigenvalue form by defining

$$u_k(\eta) = e^{i\alpha_k(\eta+1/2)} \phi_k(\eta). \quad (3.11)$$

The functions $u_k(\eta)$ satisfy

$$\Lambda_\sigma(\eta, T) u_k(\eta) = -\alpha_k u_k(\eta), \quad (3.12a)$$

subject to the boundary condition

$$u_k(\frac{1}{2}) = u_k(-\frac{1}{2}), \quad (3.12b)$$

where we define

$$\Lambda_\sigma(\eta, T) = i \frac{\partial}{\partial \eta} - T h_\sigma(\eta) \quad (3.13a)$$

and

$$h_\sigma(\eta) = \frac{p^2}{2m} - \frac{1}{2} V(0) + \int V(x-x') \sigma(x', \eta) dx'. \quad (3.13b)$$

In this representation, the α_k are the eigenvalues of Λ_σ in the space defined by (3.12b).

The functional derivative $\delta \alpha_k / \delta \sigma$ in (3.10) is simply evaluated using perturbation theory for the change of α_k when σ is changed to $\sigma + \delta \sigma$. In Ref. 5 this was done in the case of real T , which corresponded to a Hermitian Λ_σ . Allowing for general complex T , one should deal with the perturbation of a non-Hermitian Λ_σ . In the standard way, we introduce a biorthogonal set $\{u_k, v_k\}$, where u_k are solutions of (3.12) and v_k are determined by the adjoint operator

$$\Lambda_\sigma^*(\eta, T) v_k(\eta) = -\beta_k v_k(\eta), \quad (3.14)$$

$$v_k(\frac{1}{2}) = v_k(-\frac{1}{2}).$$

Obviously, for a general complex T and σ

$$\Lambda_\sigma^*(\eta, T) = i \frac{\partial}{\partial \eta} - T^* h_{\sigma^*}(\eta) \quad (3.15)$$

and

$$\beta_k^* = \alpha_k. \quad (3.16)$$

Also, we assume the normalization

$$\int_{-1/2}^{1/2} d\eta \int dx v_k^*(x, \eta) u_k(x, \eta) = 1, \quad (3.17)$$

and notice that $\int dx v_k^* u_k$ is independent of η .

From (3.12) one finds

$$\frac{\delta \alpha_k}{\delta \sigma(x, \eta)} = -\frac{\delta}{\delta \sigma(x, \eta)} \int d\eta' dx' v_k \Lambda_\sigma(\eta', T) u_k$$

$$= T \int V(x-x') v_k^*(x', \eta) u_k(x', \eta) dx', \quad (3.18)$$

where we have used

$$\frac{\delta \Lambda_\sigma(\eta')}{\delta \sigma(x, \eta)} = -TV(x-x') \delta(\eta - \eta'). \quad (3.19)$$

The variations of v_k and u_k do not contribute be-

cause of (3.17).

Inserting (3.18) in the SPA condition (3.10), one obtains

$$\sigma_0(x, \eta) = \sum_{k=1}^A v_k^*(x, \eta) u_k(x, \eta). \quad (3.20)$$

For notational simplicity, we have defined the occupation numbers such that $n_k = 1$ for $1 \leq k \leq A$, and zero otherwise. The self-consistency condition (3.20) together with Eqs. (3.12) and (3.14) define the general mean field equations for the time evolution with complex values of T .

It is easily verified that when $T = T_1$ is real, $\alpha_k = \alpha_k^*$, $u_k = v_k$, and σ_0 acquires the familiar Hartree form. In the case of a pure imaginary $T = -iT_2$, $\alpha_k = -\alpha_k^*$ is also imaginary, $v_k^*(\eta) = u_k(-\eta)$, and the mean field equations become

$$\left\{ \frac{\partial}{\partial \eta} + T_2 \left[\frac{p^2}{2m} - \frac{1}{2} V(0) + \int V(x-x') \sigma_0(x', \eta) dx' \right] \right\} \phi_k = 0, \quad (3.21a)$$

$$\sigma_0(x, \eta) = \sum_{k=1}^A \phi_k(x, \eta) \phi_k(x, -\eta), \quad (3.21b)$$

with boundary conditions

$$\phi_k(x, \eta = \frac{1}{2}) = e^{-\lambda_k} \phi_k(x, \eta = -\frac{1}{2}), \quad (3.22a)$$

where the real parameter λ_k is defined

$$\lambda_k = i \alpha_k \quad (3.22b)$$

and we have used ϕ_k rather than u_k of (3.11).

As was discussed in the preceding section, the SPA for the imaginary-time propagation describes the process of tunneling and leads to the complex poles in the trace of $(H - E)^{-1}$. We now show that the properties of Eqs. (3.21) suggest that this is also true in the present mean-field approximation for the many-nucleon problem.

We start by noticing that (3.21) represent a system of $2A$ equations for $\phi_k(\eta)$ and $\phi_k(-\eta)$ analogous to $\phi_k(t)$ and $\phi_k^*(t)$ in the real time TDHF. Continuing the analogy, it is not difficult to show that $\phi_k(\eta)$ and $\phi_k(-\eta)$ can be regarded as canonically conjugate variables and that Eqs. (3.21) are classical Hamiltonian equations with the Hamiltonian functional

$$\begin{aligned} \mathcal{H}\{\phi_k(-\eta), \phi_k(\eta)\} = & \sum_{k=1}^A \int dx \phi_k(x, -\eta) \kappa \phi_k(x, \eta) \\ & + \frac{1}{2} \sum_{k,j=1}^A \int dx dx' \phi_k(x, -\eta) \phi_j(x, \eta) \\ & \times V(x-x') \phi_j(x', -\eta) \\ & \times \phi_j(x', \eta), \quad (3.23) \end{aligned}$$

where

$$\kappa = -\frac{\nabla^2}{2m} - \frac{1}{2} V(0). \quad (3.24)$$

Clearly, since \mathcal{H} does not depend explicitly on η , it is conserved by (3.21), which can also be verified by explicit evaluation of $d\mathcal{H}/d\eta$.

Equations (3.21) possess other conserved quantities similar to ordinary TDHF, such as particle number

$$\sum_{k=1}^A \int dx \phi_k(x, \eta) \phi_k(x, -\eta) = A. \quad (3.25)$$

By the usual substitution [Eq. (3.11)] with $i\alpha_k = \lambda_k$, Eqs. (3.21) are transformed into the eigenvalue form defined in the space of functions on the interval $-\frac{1}{2} \leq \eta \leq \frac{1}{2}$ with "periodic" conditions (3.12b). Since $\sigma(\eta)$ is symmetric, $\sigma(\eta) = \sigma(-\eta)$, the operator on the left hand side of (3.12a) is Hermitian, provided the inner product is defined as

$$\int_{-1/2}^{1/2} d\eta \int dx v(x, -\eta) u(x, \eta) \quad (3.26)$$

for any two $u(x, \eta)$ and $v(x, \eta)$ satisfying Eq. (3.12b).

The set (3.21) has particular solutions closely related to the conventional HF stationary states and the random-phase approximation (RPA) excitations built upon these states. For all solutions ϵ_k and ψ_k of the static HF equations,

$$\phi_k(x, \eta) = e^{-\epsilon_k T} \psi_k(x) \quad (3.27)$$

satisfies Eq. (3.21). Furthermore, if $X_{ik}^{(\nu)}$, $Y_{ik}^{(\nu)}$, and ω_ν are solutions of the standard RPA equations, then

$$\begin{aligned} \phi_k(x, \eta) = & e^{-\epsilon_k T} \psi_k(x) \\ & + \sum_{i=A+1}^{\infty} (X_{ik}^{(\nu)} e^{-\omega_\nu T} + Y_{jk}^{(\nu)} e^{\omega_\nu T}) \psi_i(x) e^{-\epsilon_k T} \end{aligned} \quad (3.28)$$

satisfy Eq. (3.21) for infinitesimal amplitudes X and Y . It follows then that if all the eigenfrequencies ω_ν of the RPA equations are real, in which case the static HF solution is stable with respect to the TDHF evolution in *real time*, the corresponding solution to the imaginary time mean-field Eqs. (3.21) is unstable, since Eq. (3.28) does not contain i multiplying ω_ν .

Thus, the mean field approximation to the many-body problem is analogous in many respects to the simple one-dimensional problem of Sec. II. In Fig. 1 the classical solution which corresponds to a static HF solution is $q(t) = q_0$. This solution is stable with respect to the *real time* classical equations, and the frequency of small oscillations in the vicinity of q_0 corresponds to the real RPA frequencies in linearized TDHF. The classical equations in imaginary time formally describe a mo-

tion in the potential of Fig. 1 with the *reversed sign*. In such a potential, $q(t) = q_0$ is still a static solution; however, this solution is *unstable* and actually should be considered as a starting point of a trajectory which travels inside the barrier, bounces from its outer wall, and is reflected back to q_0 . Because of the infinitely small velocity near q_0 , the time period of such a bounce will be infinitely long. However, the action $\int p(dq/dt)dt$ accumulated during the bounce will be finite and provides the information on the quantum-mechanical penetrability through the barrier. The energy of the bounce is obviously equal to the energy of the static solution q_0 .

Returning to Eqs. (3.21), we observe that also in this case, a solution which has a nontrivial η dependence with *finite* derivatives $\partial\phi_k/\partial\tau$, $\tau = T_2\eta$ tends to static solutions (3.27) when $T_2 \rightarrow \infty$. The boundary conditions (3.22) suggest that this happens at both $\eta \rightarrow -\frac{1}{2}$ and $\eta \rightarrow +\frac{1}{2}$ and that $\lambda_k = \epsilon_k T_2$. Since the energy [Eq. (3.23)] of this solution is conserved, it is equal to $E_{\text{HF}}^{\text{static}}$ in analogy with the simple problem of Sec. II.

The conjecture made above about the behavior of the solutions of Eqs. (3.21) in the $T_2 \rightarrow \infty$ limit, though far from being rigorously proved here, seems to reflect a general property of classical equations in the presence of unstable equilibrium points. It pertains to all imaginary time (Euclidian) solutions to classical field equations discussed recently in the literature.³ The crucial requirement is, of course, on finite values of the derivatives $\partial\phi_k/\partial\tau$ or, equivalently, the finite action corresponding to the bounce solution [cf. Eq. (3.31)]. In the next section we present an explicit numerical example of a bounce solution in the context of a nontrivial many-body problem. Further discussion of the properties of Eqs. (3.21) can be found in Appendix B.

From Eqs. (3.7) and (3.9a) it follows that the action associated with a bounce solution is

$$S_2 = -\frac{iT_2}{2} (\sigma_0, V\sigma_0) + i \sum_{k=1}^A \lambda_k [\sigma_0], \quad (3.29)$$

with σ_0 and λ_k defined in Eqs. (3.21). Since the energy of the bounce is equal to $H_{\text{HF}}^{\text{static}}$, we can easily find the reduced action, Eq. (2.20), corresponding to the W_2 in Sec. II.

$$\begin{aligned} iW_2 &= -iE_{\text{HF}}^{\text{static}}T_2 + S_2 \\ &= -iT_2 \int_{-1/2}^{1/2} \mathcal{H} d\eta + S_2. \end{aligned} \quad (3.30)$$

Using the expression (3.22) for \mathcal{H} and Eqs. (3.21) one obtains, in terms of u_k ,

$$W_2 = \sum_{k=1}^A \int_{-1/2}^{1/2} d\eta \int u_k(-\eta) \frac{\partial u_k(\eta)}{\partial \eta} dx, \quad (3.31)$$

which is obviously finite since $u_k(\eta)$ approaches the static HF solution as $\eta \rightarrow \pm \frac{1}{2}$. One also observes that since $u_k(-\eta)$ and $u_k(\eta)$ are canonically conjugate, the expression (3.31) is of the form $\int p\dot{q}dt$.

Thus far, our discussion of spontaneous decay has assumed only one bounce solution, which evolves from the HF ground state to the classically allowed region for the evolution of separated fragments. For a nucleus with many open decay channels, there should, in general, exist distinct tunneling solutions for symmetric fission, asymmetric fission, nucleon emission, alpha decay, as well as more complicated many-body breakup. Dismissing, for the moment, problems associated with c.m. motion in mean field theories, which will complicate light particle emission, these distinct tunnelling solutions should be well-separated and thus summed independently in the SPA. Denoting by $W_2^{(a)}$ the self-consistent bounce solutions to Eqs. (3.21) evolving from the stationary HF point to the a th distinct fragment configuration, the sum of all periodic trajectories beginning in region I and comprised of any combination of cycles in regions I and II yields the contribution to the trace:

$$\sum_{k=1}^{\infty} \left[e^{iW_1} \sum_{n=0}^{\infty} \left(\sum_a e^{-W_2^{(a)}} \right)^n \right]^k = \frac{e^{iW_1}}{1 - e^{iW_1} - \sum_a e^{-W_2^{(a)}}}. \quad (3.32)$$

The sum over all periodic trajectories beginning either in region I or region II is then

$$\frac{1}{1 - e^{iW_1} - \sum_a e^{-W_2^{(a)}}} - 1. \quad (3.33)$$

If analogous bounce solutions could be joined to the same periodic TDHF solutions infinitesimally above the static HF energy, then by the arguments in Sec. II, one would obtain the total width as a sum of partial escape widths

$$\Gamma = \sum_a \Gamma^{(a)},$$

where

$$\Gamma^{(a)} = 2 \left(\frac{\partial W_1}{\partial E} \right)^{-1} e^{-W_2^{(a)}(E)}. \quad (3.34)$$

This result has the very intuitive feature of having each bounce solution determine the penetrability for the corresponding partial width, and one might well hope to understand microscopically the competition between symmetric and asymmetric fission, for example, as one progresses through a sequence of isotopes.

The action (3.31) calculated on a bounce solution defines the penetrability factor $\exp(-W_2^{(a)})$ in the

general expression (3.34) for the partial width. Although the penetrability itself only requires joining solutions at the stationary HF energy, which occurs automatically for our bounce solutions, the derivation of the pre-multiplying factor requires joining solutions in the classically allowed and forbidden regions infinitesimally above the static HF energy as well. For real values of T , solutions to Eqs. (3.12), (3.14), and (3.20) were discussed in Ref. 5. When the deviation from $E_{\text{HF}}^{\text{static}}$ is small, they are the regular RPA modes obtained from the linearization of the TDHF equations. The corresponding solutions for the imaginary T are determined by linearizing Eqs. (3.21) around the bounce solution discussed above. In order to construct a periodic solution for a general complex T it is necessary to understand how these pure real and pure imaginary solutions should be matched. Although the discussion in Appendix B suggests that the matching should occur at the generalized turning point of Eqs. (3.21), we have not yet been able to find the correct matching procedure. Because of this it was not possible to derive the expression for the preexponential factor in Eq. (3.34), and to this extent the present discussion is limited to the determination of the penetrabilities $\exp[-W_2^{(a)}(E)]$.

IV. APPLICATION TO A MODEL MANY-BODY SYSTEM

The preceding formalism is useful for nuclear physics only if bounce solutions with the properties assumed in the last section can actually be obtained for self-bound saturating many-fermion systems. Therefore, it is crucial to apply these ideas to a tractable model system embodying the essential features of finite nuclei.

Since we have been unable to find a satisfactory analytically solvable model relevant to nuclear fission, we turn to a numerically solvable problem, and for computational simplicity, restrict our attention at present to one spatial dimension. The most crucial feature of finite nuclei which must be embodied in our model is nuclear saturation; the fact that infinite nuclear matter in the absence of Coulomb forces has minimum binding energy per particle at a finite density ρ_{NM} , and that finite nuclei have density distributions which are roughly constant and approximately equal to ρ_{NM} in the interior with steep surfaces of roughly constant diffuseness. Since in the absence of Coulomb forces, the binding energy per particle of finite nuclei would monotonically approach that of nuclear matter with increasing A , aside from small shell fluctuations, it is also necessary to introduce an appropriate one-dimensional analog

of the Coulomb force to render it energetically favorable for a massive bound one-dimensional system to break up into two lighter daughters.

The simplest effective interaction applicable to a mean-field theory of real nuclei embodying these features is the modified Skyrme interaction¹² of the form used in Ref. 13. The basic attraction is provided by a short-range two-body force, the direct Coulomb force is included, and saturation is effected by means of a zero-range repulsive three-body force. The exact orthogonality of a HF theory and simplicity of a purely Hartree potential are simultaneously achieved by multiplying the finite range two-body force by the operator $P = \frac{1}{15} + \frac{4}{15} P_x$, where P_x is the space exchange operator, which makes the exchange term vanish identically for spin-isospin symmetric systems. An analogous effective interaction is therefore used to define our model problem in one spatial dimension. For convenience, we define dimensionless variables x and t such that xl_0 denotes a position, tt_0 denotes a time, and energies are expressed in units of E_0 . Once the length scale l_0 has been specified, E_0 and t_0 are defined by

$$E_0 = \frac{\hbar^2}{2ml_0^2} \quad (4.1)$$

and

$$t_0 = \frac{\hbar}{E_0}, \quad (4.2)$$

where m is the mass of the fermion. Since the only physical length in one-dimensional nuclear matter is specified by the saturation density, we will define $l_0 \equiv 1/\rho_{\text{NM}}$. For comparison, if one defined analogous units in three dimensions such that $\rho_{\text{NM}} = 0.16 \text{ fm}^{-3} \equiv 1/l_0^3$, we would have $l_0 = 1.85 \text{ fm}$, $E_0 = 6.03 \text{ MeV}$, and $t_0 = 1.09 \times 10^{-22} \text{ s}$. With units of l_0 , E_0 , and t_0 understood, the Hamiltonian density for a determinantal wave function in our one-dimensional model problem is

$$\begin{aligned} \mathcal{H}[\bar{\phi}(x,t), \phi(x,t)] = & -M \sum_{\alpha} \bar{\phi}_{\alpha}(x,t) \frac{\partial^2}{\partial x^2} \phi_{\alpha}(x,t) \\ & + \frac{1}{2} \int dx' \rho(x,t) V(x-x') \rho(x',t) \\ & + \frac{1}{3} V_3 \rho^3(x,t), \end{aligned} \quad (4.3a)$$

where

$$V(x) = \sum_{j=1}^2 \frac{V_j}{\sqrt{\pi}\gamma_j} e^{-x^2/\gamma_j^2}, \quad (4.3b)$$

$$\rho(x,t) = M \sum_{\alpha} \bar{\phi}_{\alpha}(x,t) \phi_{\alpha}(x,t), \quad (4.3c)$$

and

$$\bar{\phi}_{\alpha}(x,t) = \begin{cases} \phi_{\alpha}^*(x,t) & \text{for real time solutions} \\ \phi_{\alpha}(x,-t) & \text{for tunneling solutions.} \end{cases} \quad (4.3d)$$

M denotes the spin degeneracy chosen to be 4 to simulate the spin-isospin degeneracy of nuclei, and \sum_{α} denotes a sum over all occupied spatial orbitals. Values of the parameters in Eq. (4.3) are given in Table I. The attractive Gaussian potential represents the attractive binding nuclear interaction, and the very long range repulsive Gaussian is intended to simulate the effect of the repulsive Coulomb potential.

The binding energy per particle of uniform matter of density ρ in the absence of the Coulomb-type potential V_2 is

$$E/N = \frac{1}{3} \left(\frac{\pi}{M} \right)^2 + \frac{1}{2} V_1 \rho + \frac{1}{3} V_3 \rho^2, \quad (4.4)$$

which yields the nuclear matter binding energy per particle

$$E/N|_{\text{NM}} = -\frac{3}{16} \frac{V_1^2}{[(\pi/M)^2 + V_3]} = -0.372 \quad (4.5)$$

at the saturation density

$$\rho_{\text{NM}} = \frac{3}{4} \frac{V_1}{[(\pi/M)^2 + V_3]} = 1. \quad (4.6)$$

At equilibrium, the potential energy per particle, $-0.578E_0$, is somewhat greater in magnitude than the kinetic energy per particle of $0.206E_0$, in qualitative agreement with ordinary nuclear matter.

Finite bound states are determined by solving the static HF equations arising from the Hamiltonian density in Eq. (4.3):

$$\left[\frac{d^2}{dx^2} + \int V(x-x')\rho(x')dx' + V_3\rho^2(x) \right] u_{\alpha}(x) = \epsilon_{\alpha} u_{\alpha}(x). \quad (4.7)$$

The resulting density distributions and binding energies are presented for $A=4, 8$, and 16 particles in Fig. 2 and Table II, respectively. Clearly these solutions possess the properties specified above for our one-dimensional model system. As A increases, the position of the surface of roughly constant diffuseness increases linearly in A , while the interior density is approximately constant and is displaced slightly below the value $\rho_{\text{NM}}=1$ by the presence of the Coulomb-type potential V_2 . The maximum binding energy per particle in the per-

TABLE I. Values of the parameters appearing in Eq. (4.3) for the one-dimensional nuclear model.

M	4
γ_1	2
γ_2	10
v_1	-1.489
v_2	0.40
v_3	0.5

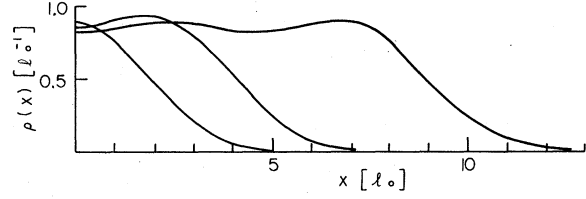


FIG. 2. Hartree-Fock density distributions for 4-, 8-, and 16-, particle systems. Since solutions are symmetric about $x=0$, distributions are only shown for positive x .

iodic table occurs near $A=8$, so that a 16-particle system is unstable with respect to fission into two 8-particle daughters which, in turn, are stable against further fission into 4-particle granddaughters.

Before presenting the bounce solution describing spontaneous decay in this model, it will prove useful to discuss briefly the static constrained HF problem for this system. An immediate problem in generalizing the discussion associated with Fig. 1 to the present many-body problem is what quantity plays the role of $V(q)$ and how to deal with the infinite number of coordinates. Since the equations of motion are the Hamiltonian equations associated with $\mathcal{H}[\bar{\phi}(x,t), \phi(x,t)]$ in Eq. (4.3), one would ideally like to determine $\mathcal{H}[\bar{\phi}(x), \phi(x)]$ for a family of determinants which continuously deform through a series of shapes from the HF ground state to the saddle point and on to the scission configuration. One practical way to do this is to calculate the constrained HF energy of deformation surface. Instead of solving the static HF problem, one minimizes the quantity

$$\mathcal{H}_{\lambda}^c = \mathcal{H}[\phi(x), \phi(x)] + \sum_i \frac{\lambda_i}{2} \{Q_0^i - Q^i[\phi(x)]\}^2, \quad (4.8a)$$

where

$$Q^i[\phi(x)] = M \sum_{\alpha} \int dx \phi_{\alpha}(x) Q^i(x) \phi_{\alpha}(x). \quad (4.8b)$$

In this way, determinants may be constrained to have arbitrary expectation values of relevant operators $Q^i(x)$. For symmetric fission of a 16-par-

TABLE II. Ratio of binding energy per particle in finite nuclei to that in nuclear matter for three model nuclei.

A	$\frac{E(A)}{A} / \left(\frac{E}{A} \right)_{\text{NM}}$
4	0.574
8	0.619
16	0.583

ticle system in our one-dimensional model, it is sufficient to consider the single variable $Q = x^2$, and a plot of values of $\mathcal{H}[\phi(Q_0)]$ vs $Q[\phi(Q_0)]$ for a range of Q_0 yields the deformation energy as a function of $\langle x^2 \rangle$ shown in Fig. 3. The maxima and minima of this constrained energy of deformation curve correspond to exact stationary solutions of the HF equations, while the rest of the curve smoothly interpolates between these unique stationary points. If one introduced other appropriate variables to constrain, for example, asymmetry and geometry of neck formation, one would obtain a multidimensional surface in which the essential topology of ridges and valleys would be determined by the maxima, minima, and saddle points, which are unique stationary points of the unconstrained problem. One technical observation which is crucial to the numerical solution of the subsequent bounce equation is the fact that unstable stationary HF solutions, such as the saddle point denoted by (b) in Fig. 3, cannot be calculated iteratively except by the addition of a suitable constraint. If one selected an initial determinant arbitrarily close to point (b) and iterated the unconstrained equations, the solution would ultimately approach the 16-particle quasistable state corresponding to the local minimum at (a) or the HF ground state for two separated fragments of mass 8. Conversely, the fact that one converges to a saddle point solution with only one constraint conclusively proves that the multidimensional energy surface is not concave downward in any other direction.

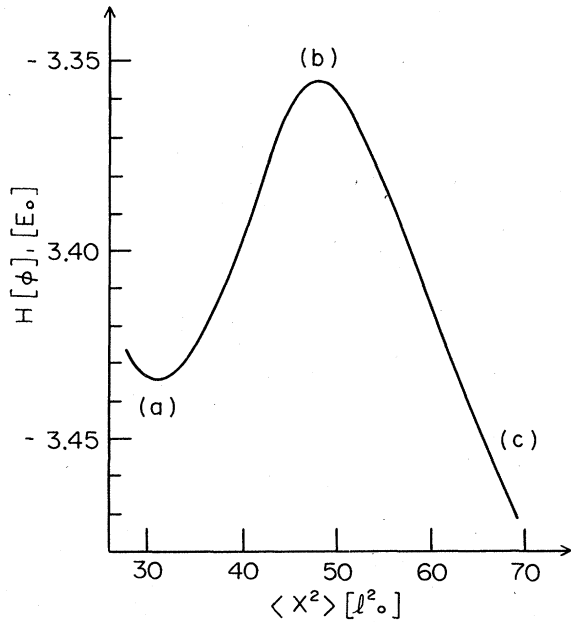


FIG. 3. Constrained energy of deformation curve for $A = 16$ fission barrier.

The mean-field equations of motion for a bounce solution in the tunneling regions for the model defined in Eq. (4.3) may be written as

$$\left[\frac{\partial}{\partial \eta} + T \left(-\frac{\partial^2}{\partial x^2} + \int V(x-x')\rho(x', \eta)dx' + V_3\rho^2(x, \eta) \right) \right] \times u_\beta(x, \eta) = \lambda_\beta u_\beta(x, \eta) \quad (4.9a)$$

with boundary condition

$$u_\beta(x, \frac{1}{2}) = u_\beta(x, -\frac{1}{2}) \quad (4.9b)$$

or

$$-\frac{\partial \phi_\beta(x, \eta)}{\partial \eta} = T \left(-\frac{\partial^2}{\partial x^2} + \int V(x-x')\rho(x', \eta)dx' + V_3\rho^2(x, \eta) \right) \phi_\beta(x, \eta) \quad (4.10a)$$

with the boundary condition

$$\phi_\beta(x, \frac{1}{2}) = e^{-\lambda_\beta} \phi_\beta(x, -\frac{1}{2}), \quad (4.10b)$$

where

$$u_\beta(x, \eta) = e^{\lambda_\beta(\eta+1/2)} \phi_\beta(x, \eta), \quad (4.11a)$$

$$\begin{aligned} \rho(x, \eta) &= M \sum_\beta u_\beta(x, -\eta) u_\beta(x, \eta) \\ &= M \sum_\beta \phi_\beta(x, -\eta) \phi_\beta(x, \eta), \end{aligned} \quad (4.11b)$$

and a new time variable is defined as in Sec. III,

$$\eta = t/T. \quad (4.11c)$$

The kinetic energy term and two-body force contributions follow directly from Eqs. (3.12) and (3.21). The three-body force contribution is derived in Appendix C where the Hubbard-Stratonovich transformation is applied twice to the term

$$\exp \left[-i(V_3/3) \int \rho^3(x, t) dx dt \right],$$

and the resulting expression is approximated by the SPA.

Several salient features of evolution in complex time are evident from Eqs. (4.9) and (4.10). The real-time counterpart of Eq. (4.10a) has an additional factor of $-i$ in the left hand side so that the wave function ϕ at any two times is related by a unitary operator. As consequences, orthonormal wave functions remain orthonormal, a static HF wave function simply acquires a time-dependent phase factor, and a coherent velocity field is described by the phase factor $e^{i\theta(x)}$, where $v(x) = (\hbar/m)(d\theta/dx)$. Although none of these properties pertain for the imaginary-time equation (4.10), and simple phase factors are replaced by growing or decaying exponentials, nevertheless, physical quantities remain sensible through the symmetrical appearance of $\phi(x, -\eta)$ and $\phi(x, \eta)$. Thus, even though individual wave functions grow or

decay exponentially in time, the combination $\int dx \phi_\alpha(x, -\eta)\phi_\beta(x, \eta)$ is time-independent and $\rho(x, \eta)$ remains properly normalized. Similarly, even though an individual bounce wave function which travels first to the right and then back to the left might appear to be seriously distorted spatially by the real factor $e^{s(x)}$, again compensating factors of $e^{s(x)}$ and $e^{-s(x)}$ cancel out of the bilinear combination appearing in ρ . Although the physics usually associated with unitarity in TDHF equations is thus retained by Eqs. (4.9) and (4.10), the numerical difficulties associated with the solution of Eq. (4.10) are significantly different than in the corresponding real-time case. All computational aspects of the solution presented in this section are relegated to Appendix C.

The easiest way to think about iterative solutions to the bounce equations is to view Eq. (4.9) as a two-dimensional generalization of the corresponding one-dimensional static Hartree equations. Ignoring the η dependence for a specified function $\rho(x)$, Eq. (4.9) is a one-dimensional eigenvalue problem defined by a second-order differential equation, and the associated two boundary conditions that u vanish at the two edges of a large box. Even though little is known mathematically about the solution to such self-consistent equations, starting from a given density $\rho(x)$, one may solve for the single particle wave functions $u_\alpha(x)$, construct a new density from these u 's, and iterate until the sequence converges to the self-consistent $\rho(x)$ which is in some sense closest to the original guess. Adding the first derivative with respect to η in Eq. (4.9) and the boundary condition (4.9b) that the wave function be periodic in time, simply generates an analogous two-dimensional self-consistent problem, which again may be expected to converge to the stable self-consistent solution closest to the initial guess $\rho(x, \eta)$.

As has already been discussed, an initial guess $\rho(x)$ for the one-dimensional Hartree problem arbitrarily close to the saddle point (b) will not converge to the saddle point stationary solution unless one adds a constraint. Similarly, we have found that even if one begins with an initial density $\rho(x, \eta)$ arbitrarily close to the exact bounce solution, which begins at the HF solution (a) at $\eta = -\frac{1}{2}$, passes through the saddle point (b), reaches the turning point (c) at $\eta = 0$, and then returns to the HF solution (a) $\eta = \frac{1}{2}$, unless one imposes a constraint, the solution will eventually converge to a time-independent 16-particle static HF solution or two static 8-particle daughters. Thus, the bounce, like the saddle point stationary solutions, has one unstable degree of freedom, and one must therefore add to the potential terms in Eqs. (4.9) or (4.10a) a constraint, which we took of the form

$$V_\lambda(x) = \lambda \left[\int_{-1/2}^{1/2} d\eta \int x'^2 \rho(x', \eta) dx' - x_0^2 \right] x^2. \quad (4.12)$$

Regarding the resulting self-consistent solutions $\rho_{x_0}(x, \eta)$ as functions of the parameter x_0 , the bounce solution corresponds to that x_0 for which

$$\int_{-1/2}^{1/2} d\eta \int dx' x'^2 \rho(x', \eta) = x_0^2, \quad (4.13)$$

i.e., that value of x_0 for which the constraint vanishes. Thus the constraint renders the system stable with respect to small deviations away from the bounce without altering the bounce solution itself.

Bounce solutions for symmetric fission of a 16-particle system into two fragments are shown in Figs. 4 and 5. Figure 4 shows the density distribution $\rho(x, \eta_i)$ for six evenly spaced intervals from $-\frac{1}{2}$ to 0. The top density is identical to the exact static HF distribution, and one observes that most of the shape deformation is localized in a small time interval near $\eta = 0$.

Further insight into the behavior of the Slater determinant is provided by the single-particle wave functions graphed at $\eta = -\frac{1}{2}$ and $\eta = 0$ in Fig. 5. The left-hand wave functions are clearly just the first four eigenfunctions of the 16-particle HF potential well. The right-hand wave functions correspond approximately to even and odd combinations of the lowest two wave functions in two nearly separated 8-particle wells. Hence, a more illuminating way to think about the determinant of these wave functions is to consider a different repre-

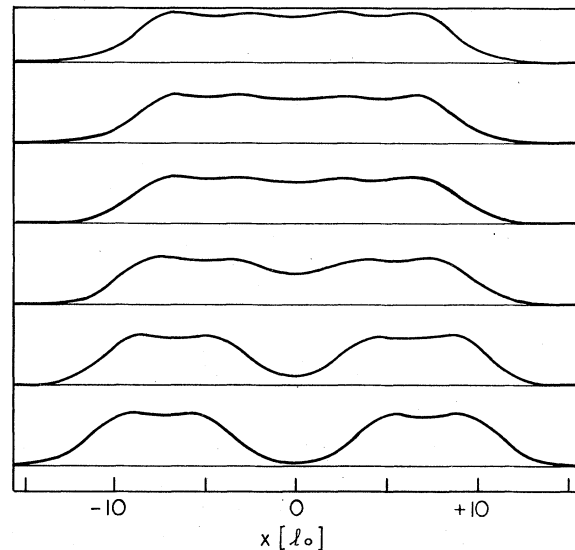


FIG. 4. Density profiles for $A = 16$ bounce solution in evenly spaced intervals from $\eta = -\frac{1}{2}$ to $\eta = 0$ in time increments of $20t_0$.

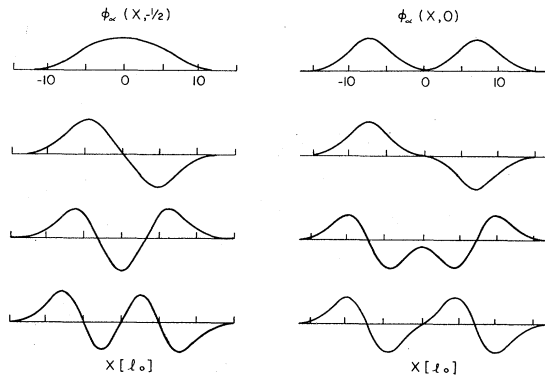


FIG. 5. Normalized self-consistent bounce wave functions at times $\eta = -\frac{1}{2}$ and at $\eta = 0$.

sensation comprised of the sums and differences of the first two and last two functions. To the extent to which two wave functions are then localized on the left and the other two on the right, the determinant approximately factorizes into the product of two determinants describing two 8-particle daughters. Thus, one observes that the bounce solution for this one-dimensional model manifests all the required physical properties of our formalism. At large positive and negative times, it indeed joins the 16-particle HF solution, and near time zero is evolved self-consistently through the barrier to obtain a turning point configuration corresponding to two nearly separated 8-particle fragments.

This turning point configuration can presumably be used as the initial condition of the *real-time* TDHF equations, which may provide information on the development of the fragments on their way from the turning point to the asymptotic region of complete separation. However, it is important that the knowledge of the imaginary-time bounce solution is already sufficient for the calculation of the penetrability [Eq. (3.31)].

V. CONCLUSION

In this work, we have presented a mean-field theory of the tunneling decay of nuclear many-body systems. We have applied the SPA to a well-behaved quantity containing the physical information concerning all possible decay channels without having to specifically define reaction channels, and have shown that the leading approximation to the sum of partial widths depends only upon a discrete set of periodic bounce solutions to TDHF-like equations in complex time. In principle, this theory should contain a wealth of information concerning the competition of alternative decay channels for a wide variety of nuclei.

The formalism has been applied to a model sys-

tem of nuclei in one spatial dimension. Explicit solutions for the symmetric fission of a 16-particle system into two 8-particle daughters have demonstrated the feasibility of numerically solving the resulting self-consistent integrodifferential equations and have verified that the bounce solution has the conjectured long-time behavior. Aside from the immediate application, the one-dimensional model presented in this work offers many opportunities for future research. In addition to exploring asymmetric fission and investigating other particle numbers, the system provides an ideal testing ground for many approximations currently applied to fission. For example, one way of comparing mass parameters for any prescription of collective coordinates (or inertial tensors for many degrees of freedom) is to differentially equate the penetrability factors:

$$\int_0^{1/2} d\eta \int dx \sum_{\alpha} u_{\alpha}(x, -\eta) \frac{\partial}{\partial \eta} u_{\alpha}(x, \eta) = \int_{q_1}^{q_2} \{2M(q)[V(q) - E]\}^{1/2} dq.$$

Despite the potential promise of the present theory of tunneling, a number of formal and practical problems remain. One obvious formal problem is the joining of solutions at the interface between classically allowed and forbidden regions which was discussed in detail in the text. Center of mass motion is always a problem in mean field theories, and is especially troublesome in the present case in which many decays of interest involve light fragments. Clearly, $1/A$ c.m. motion errors will be catastrophic in dealing with nucleon, deuteron, and alpha emission. Similarly, description of the fission of ${}^8\text{Be}$ into two α particles is hopeless when the actual Q value is in kilovolts, while the spurious c.m. energy of two alpha particles is roughly 16 MeV higher than the spurious c.m. energy of ${}^8\text{Be}$. Other problems already encountered in our previous investigation of large amplitude collective motion,⁵ such as evaluating corrections to the SPA and consistently deriving an effective interaction, are equally relevant to this present work.

Aside from these formal problems, a number of practical difficulties arise in considering the application of this theory to real nuclei in three dimensions. The computational difficulty is obviously far greater than the corresponding three-dimensional static HF problem because of the addition of the fourth time variable. In addition, it is clear from the earlier mean-field treatment of induced fission¹⁴ that the breaking of axial symmetry by the mean field plays a crucial role in fission dynamics, so it is essential to use a fully three-dimensional rather than axially symmetric

wave function. Finally, spontaneous fission is strongly influenced by shell effects, which, in turn, necessitate the inclusion of a spin-orbit force, thereby severely escalating the numerical problem.

Thus, for initial investigations, it appears prudent to treat light systems in which one artificially increases the charge of the proton to obtain fissilities characteristic of actinide nuclei. Incorporating a number of obvious improvements over the brute force methods employed in this work, satisfactory bounce solutions for nuclei from ${}^8\text{Be}$ to ${}^{32}\text{S}$ have been obtained with very modest computer times,¹⁵ and a number of fruitful investigations are clearly feasible in these systems. Depending upon the future improvements in numeri-

cal methods, the adaptability of sparse matrix problems to array processing, and the availability of computer resources, it may eventually prove feasible to apply the theory presented in this work to a realistic calculation for uranium.

ACKNOWLEDGMENTS

We are grateful to A. K. Kerman for many stimulating discussions and suggestions concerning this work. Discussions with F. Coester, F. Lenz, and E. Moniz were helpful in bringing the work to its present form. This work was supported in part through funds provided by the U. S. Department of Energy (DOE) under Contract No. DE-AC02-76ERO-3069.

APPENDIX A. EVALUATION OF THE SMOOTHED DENSITY OF STATES

Following Ref. 16 we evaluate the smoothed density of states in a finite box of length L

$$\rho_\gamma(E) = \frac{1}{\pi} \text{Im Tr}(H - E - i\gamma)^{-1}. \quad (\text{A1})$$

The discrete states in the box are smoothed with a Lorentzian width γ , large compared to the level spacing

$$\gamma = g \frac{\pi}{L} \left(\frac{2E}{m} \right)^{1/2}, \quad g \gg 1, \quad (\text{A2})$$

but small relative to the physical width of the metastable state. Thus, we no longer attempt to approximate the individual (real) eigenvalues of H , but rather approximate the smooth, averaged quantity $\rho_\gamma(E)$. Evaluating the trace $\text{Tr}(H - E - i\gamma)$ by calculating the sum over all trajectories beginning in any of the three regions, and containing all combinations of cycles in each region yields

$$\begin{aligned} & \sum_{k=1}^{\infty} \left[e^{iW_1} \sum_{m=0}^{\infty} \left(e^{-W_2} \sum_{n=0}^{\infty} e^{iW_3} \right)^m \right]^k + \sum_{m=1}^{\infty} \left(\sum_{n=0}^{\infty} e^{inW_1} e^{-W_2} \sum_{p=0}^{\infty} e^{ipW_3} \right)^m + \sum_{l=1}^{\infty} \left[e^{iW_3} \sum_{m=0}^{\infty} \left(e^{-W_2} \sum_{n=0}^{\infty} e^{iW_1} \right)^m \right]^l \\ & = \frac{e^{iW_1} + e^{-W_2} + e^{iW_3} - 2e^{i(W_1+W_3)}}{(1 - e^{iW_1})(1 - e^{iW_3}) - e^{-W_2}}, \quad (\text{A3}) \end{aligned}$$

where, of course, W_1 , W_2 , and W_3 are evaluated at energy $E + i\gamma$.

Now we are in a position to demonstrate that region III contributes negligibly to the physical width Γ . In the limit of large L , the small imaginary part γ contributes negligibly to W_1 and W_2 . However, since the potential vanishes beyond some point q_m in region III,

$$\begin{aligned} W_3 &= \int_{q_3}^{q_m} \{2m[E + i\gamma - V(q)]dq\}^{1/2} \\ &+ [2m(E + i\gamma)]^{1/2}(L - q_m), \quad (\text{A4}) \end{aligned}$$

so that, using Eq. (A2),

$$\text{Im}W_3 \underset{L \rightarrow \infty}{\sim} (m/2E)^{1/2} \gamma L \sim g\pi \quad (\text{A5})$$

and $e^{iW_3} \sim e^{-g\pi}$. Thus, the contributions of cycles

in region III may be rendered arbitrarily small by choosing a suitable averaging width γ . The remaining terms in Eq. (A3) are identical to Eq. (2.22), and we obtain

$$\begin{aligned} \rho_\gamma(E) &\sim \text{Im} \frac{e^{iW_1} + e^{-W_2}}{1 - e^{iW_1} - e^{-W_2}} \\ &= \frac{\sin W_1}{(\frac{1}{2}e^{-W_2})^2 + (\sin \frac{1}{2}W_2)^2}. \quad (\text{A6}) \end{aligned}$$

As before, this expression defines resonances at energies

$$W_1(E_N) = 2\pi N \quad (\text{A7})$$

and with widths

$$\Gamma_N = 2 \left(\frac{\partial W_1}{\partial E} \right)^{-1} e^{-W_2(E_N)}. \quad (\text{A8})$$

APPENDIX B. PROPERTIES OF THE IMAGINARY-TIME MEAN-FIELD EQUATIONS

The equations of the real-time Hartree theory have the classical Hamilton form with canonical coordinates $\phi_k(x)$, momenta $i\phi_k^*(x)$, and Hamiltonian

$$\mathcal{H}\{i\phi_k^*, \phi_k\} = \frac{1}{2m} \sum_{k=1}^A \int dx |\nabla\phi_k|^2 + \frac{1}{2} \sum_{k,j=1}^A \int dx dx' |\phi_k(x)|^2 V(x-x') |\phi_j(x)|^2. \quad (\text{B1})$$

Performing a canonical transformation

$$\begin{aligned} \phi_k &= \sqrt{\rho_k} e^{-ix_k}, \\ \phi_k^* &= \sqrt{\rho_k} e^{ix_k}, \end{aligned} \quad (\text{B2})$$

with new coordinates

$$\rho_k = \phi_k \phi_k^* \quad (\text{B3})$$

and momenta

$$\chi_k = \frac{i}{2} (\ln\phi_k - \ln\phi_k^*), \quad (\text{B4})$$

transforms the Hamiltonian (B1) into

$$\mathcal{H}\{\chi_k, \rho_k\} = \frac{1}{2m} \sum_{k=1}^A \int \rho_k (\nabla\chi_k)^2 dx + \mathcal{V}(\rho), \quad (\text{B5})$$

where

$$\mathcal{V}(\rho) = \frac{1}{8m} \sum_{k=1}^A \int \frac{(\nabla\rho_k)^2}{\rho_k} dx + \frac{1}{2} \sum_{k,j=1}^A \int \rho_k V\rho_j dx dx'. \quad (\text{B6})$$

In this representation the two terms in (B5) are conveniently interpreted as effective kinetic and potential energies of this classical system.

As was indicated in Sec. II, the continuation of classical equations in imaginary time amounts to reversing the sign of the potential energy or, more precisely, in changing the relative signs of the kinetic and potential terms. We will now show that

this is also true for the imaginary time Hartree system described by the Hamiltonian (3.23) of Sec. III.

In imaginary time the canonical transformation of the *real* variables $\phi_k(\eta)$ and $\phi_k(-\eta)$, which is analogous to (B2), is given by

$$\begin{aligned} \phi_k(\eta) &= [\rho_k(\eta)]^{1/2} e^{-x_k(\eta)}, \\ \phi_k(-\eta) &= [\rho_k(\eta)]^{1/2} e^{x_k(\eta)}, \end{aligned} \quad (\text{B7})$$

with new coordinates

$$\rho_k(\eta) = \phi_k(\eta)\phi_k(-\eta) = \rho_k(-\eta) \quad (\text{B8})$$

and momenta

$$\chi_k(\eta) = -\frac{1}{2} [\ln\phi_k(\eta) - \ln\phi_k(-\eta)] = -\chi_k(-\eta). \quad (\text{B9})$$

In terms of $\rho_k(\eta)$ and $\chi_k(\eta)$, the Hamiltonian (3.23) becomes

$$\mathcal{H}\{\chi_k, \rho_k\} = -\frac{1}{2m} \sum_{k=1}^A \int \rho_k (\nabla\chi_k)^2 dx + \mathcal{V}(\rho), \quad (\text{B10})$$

where $\mathcal{V}(\rho)$ has the same functional form as Eq. (B6). In Eq. (B10) we omitted the additive constant term $\frac{1}{2} V(0)$ from Eq. (3.24). One observes that the transformation to imaginary time indeed reverses the relative signs of the effective kinetic and potential terms¹⁷ as compared to the real time expression (B5).

The transformation (B7) is also useful in interpreting the periodic condition (3.22a). Using the symmetry properties of $\rho_k(\eta)$ and $\chi_k(\eta)$ given by Eqs. (B8) and (B9) this condition becomes $2\chi_k(\eta = \frac{1}{2}) = \lambda_k$ so that $\nabla\chi_k(\pm\frac{1}{2}) = 0$. This means that the kinetic term in Eq. (B10) vanishes at $\eta = \pm\frac{1}{2}$, and therefore the condition (3.22a) is simply a requirement that the bounce solution starts and ends at the turning point of the Hamiltonian (B10), i.e., where its kinetic term vanishes. This observation suggests that the matching of the real time periodic mean field solution to the tunneling solution in imaginary time occurs at the turning point of the real time Hamiltonian (B5) where $\nabla\chi_k$ vanishes in the kinetic term of Eq. (B5).

APPENDIX C. FUNCTIONAL INTEGRAL REPRESENTATION FOR THREE-BODY FORCES

To treat terms in the Hamiltonian containing powers of $\hat{\rho}$ greater than two, the Hubbard-Stratonovich transformation may be applied sequentially. Expressions containing even powers may be reduced by writing

$$\exp\left(-i \int \hat{\rho}^{2n}\right) = \int D\phi \exp\left(i \int \phi^{2n}\right) \exp\left(-2i \int \phi^n \hat{\rho}^n\right) \quad (\text{C1})$$

and expressions containing odd powers may be reduced by writing

$$\begin{aligned} \exp(-i\hat{\rho}^{2n+1}) &= \exp[-(i/2)(\hat{\rho}^n + \hat{\rho}^{n+1})^2] \exp[(i/2)\hat{\rho}^{2n}] \exp[(i/2)\hat{\rho}^{2(n+1)}] \\ &= \int D\chi \exp[(i/2)\chi^2] \exp[-i(\hat{\rho}^n + \hat{\rho}^{n+1})\chi] \exp[(i/2)\hat{\rho}^{2n}] \exp[(i/2)\hat{\rho}^{2(n+1)}] \end{aligned} \quad (\text{C2})$$

and using Eq. (C1). Successive application of Eqs. (C1) and (C2) ultimately results in an exponential linear in $\hat{\rho}$.

For the three-body delta function interaction contained in Eq. (4.3), Eqs. (C1) and (C2) yield

$$\begin{aligned} \exp\left[-i(V/3) \int \hat{\rho}^3\right] &= \exp\left[-i(V/6) \int (\hat{\rho} + \hat{\rho}^2)^2\right] \exp\left[i(V/6) \int \hat{\rho}^4\right] \exp\left[i(V/6) \int \hat{\rho}^2\right] \\ &= \int D\chi \int D\phi \exp\left[i(V/6) \int (\chi^2 - \phi^2)\right] \exp\left[-i(V/3) \int \chi \hat{\rho}\right] \exp\left\{-i(V/3) \int [\chi - \phi - 1/2] \hat{\rho}^2\right\} \\ &= \iiint D\chi D\phi \bar{D}\sigma [\det(\chi - \phi - \frac{1}{2})]^{1/2} \exp\left[i(V/6) \int (\chi^2 - \phi^2 - \sigma^2 + 2\chi\sigma^2 - 2\phi\sigma^2)\right] \\ &\quad \times \exp\left[-i(V/3) \int (2\chi\sigma - 2\phi\sigma - \sigma + \chi)\hat{\rho}\right], \end{aligned} \quad (C3)$$

where the integrals appearing in the exponents are with respect to x and η , and $\bar{D}\sigma$ denotes all contributions to the measure for the σ integration which are independent of χ and ϕ . Ordering with respect to η is implied in (C3), which allows for the free manipulation of the noncommuting operators $\hat{\rho}(x, \eta)$. Carrying through the steps in the derivation subsequent to Eq. (3.4), one observes that Λ_σ contains the additional three-body contribution

$$\Lambda_\sigma^{(3)} = -\frac{TV}{3} (2\chi\sigma - 2\phi\sigma - \sigma + \chi). \quad (C4)$$

Noting that only the exponent is to be made stationary and that the premultiplying factor $[\det(\chi - \phi - \frac{1}{2})]^{1/2}$ is not varied, application of the SPA to the integrals over χ , ϕ , and σ requires that the quantity

$$i(TV/6) \int (\chi^2 - \phi^2 - \sigma^2 + 2\chi\sigma^2 - 2\phi\sigma^2) - i \sum_k \alpha_k \quad (C5)$$

be simultaneously stationary with respect to variations in χ , ϕ , and σ . The resulting equations for the stationary functions χ_s , ϕ_s , and σ_s are

$$(TV/3)(\chi_s + \sigma_s^2) = \sum_k \frac{\delta \alpha_k}{\delta \chi} = \frac{TV}{3} (2\sigma_s + 1)\sigma_0, \quad (C6a)$$

$$(TV/3)(-\phi_s - \sigma_s^2) = \sum_k \frac{\delta \alpha_k}{\delta \phi} = \frac{TV}{3} (-2\sigma_s)\sigma_0, \quad (C6b)$$

and

$$(TV/3)(-\sigma_s + 2\chi_s\sigma_s - 2\phi_s\sigma_s) = \sum_k \frac{\delta \alpha_k}{\delta \sigma} = \frac{TV}{3} (2\chi_k - 2\phi_k - 1)\sigma_0, \quad (C6c)$$

where σ_0 is the self-consistent density defined by Eq. (3.21b) and χ_s , and ϕ_s , σ_s , and σ_0 are understood to be functions of x and η . The solution of the set of equations (C6) is

$$\chi_s = \sigma_0 + \sigma_0^2, \quad (C7a)$$

$$\phi_s = \sigma_0^2, \quad (C7b)$$

$$\sigma_s = \sigma_0, \quad (C7c)$$

so that the three-body contribution to the mean field, Eq. (C4), becomes

$$\Lambda_\sigma^{(3)} = -TV\sigma_0^2, \quad (C8)$$

from which Eq. (4.9) follows immediately. Finally, as in the two-body case, we note that the SPA to Eq. (C3) yields the proper three-body total energy for the self-consistent TDHF wave function, since

$$\begin{aligned} \exp\left[i(V/6) \int (\chi_s^2 - \phi_s^2 - \sigma_s^2 + 2\chi_s\sigma_s^2 - 2\phi_s\sigma_s^2)\right] \left\langle \Psi_{\text{TDHF}} \left| T_\eta \exp\left[-i(V/3) \int (2\chi_s\sigma_s - 2\phi_s\sigma_s - \sigma_s + \chi_s)\hat{\rho}\right] \right| \Psi_{\text{TDHF}} \right\rangle \\ = \exp\left[i(2V/3) \int \sigma_0^3\right] \left\langle \Psi_{\text{TDHF}} \left| T_\eta \exp\left(-iV \int \sigma_0^2 \hat{\rho}\right) \right| \Psi_{\text{TDHF}} \right\rangle \end{aligned} \quad (C9)$$

and the premultiplying factor exactly removes the overcounting of potential energy in the single-particle equations.

APPENDIX D. NUMERICAL SOLUTION OF THE BOUNCE EQUATIONS

Due to the simplicity of the model in one spatial dimension presented in Sec. IV, the self-consistent imaginary-time mean-field equations were solved by a straightforward generalization of the standard techniques to evolve solutions of the real-time TDHF equations, with no attempt to obtain optimal stability or efficiency. The single-particle wave functions were constrained to be symmetric and discretized on an N -point spatial mesh of spacing Δx . A five-point approximation was made to the derivative appearing in

$$h[\rho] = T \left[-\frac{\partial^2}{\partial x^2} + \int V(x-x')\rho(x',\eta)dx' + V_3\rho^2(x,\eta) + V_\lambda(x) \right] \quad (D1)$$

and a single-particle wave function was evolved for J time steps of size $\Delta\eta = 1/J$ by expanding the approximate evolution operator

$$\phi_\beta(x, \eta + \Delta\eta) = \exp\left(-h\left[\frac{1}{2}[\rho(\eta) + \rho(\eta + \Delta\eta)]\right]\Delta\eta\right)\phi_\beta(x, \eta) \quad (D2)$$

in an L term Taylor series.

For a given density $\rho(x_i, \eta)$, Eqs. (4.10) were solved by evolving N independent wave functions

$$\chi_i(x_j, \eta = -\frac{1}{2}) = \delta_{ij} \quad (D3)$$

for J time steps to $\eta = \frac{1}{2}$.

Expanding each eigenfunction ϕ_β in this complete set of states

$$\phi_\beta(x_i, \eta) = \sum_n A_n^{(\beta)} \chi_n(x_i, \eta), \quad (D4)$$

the boundary condition, Eq. (4.10b), yields the eigenvalue equation

$$M_{in} A_n^{(\beta)} = \epsilon^{(\beta)} A_i^{(\beta)}, \quad (D5a)$$

where

$$M_{in} = \chi_n(x_i, \eta = \frac{1}{2}), \quad (D5b)$$

and

$$\epsilon^{(\beta)} = e^{-\lambda_\beta}. \quad (D5c)$$

A new density for an A -particle system was computed by evaluating

$$\rho(x_i, \eta) = M \sum_\beta \phi_\beta(x_i, -\eta)\phi_\beta(x_i, \eta), \quad (D6)$$

where β runs over the A/M lowest values of λ_β in Eq. (D5c).

After careful tests of precision, the final results quoted in the text were obtained with $N=12$ spatial mesh points, $J=50$ time steps, a spatial grid $\Delta x = 1.5$, a time step $T\Delta\eta = 2.$, and $L=10$ terms in the expansion of Eq. (D2). Excellent convergence was obtained in 50 iterations. Since the bounce rigorously approaches the stationary HF solution only as $T \rightarrow \infty$, and thus the energy of the bounce $H[\phi]$ only approaches E_{HF} in this limit, it is useful to note how rapidly $H[\phi]$ approaches the static value in practice. For $T=80t_0$, corresponding to 40 time steps, $H[\phi] = 3.4331E_0$, whereas for $T=100t_0$, $H[\phi] = 3.4349E_0$, agreeing precisely with E_{HF} to 5 significant figures.

*Present address: Department of Physics and Astronomy, Tel Aviv University, Ramat Aviv, Tel Aviv, Israel.

¹C. W. Wong, Phys. Rep. **15**, 283 (1974).

²M. Baranger and M. Veneroni, Ann. Phys. (N.Y.) **114**, 123 (1978).

³S. Coleman, *The Uses of Instantons*, Proceedings of the 1977 International School of Subnuclear Physics, "Ettore Majorana," Erice, Italy, 1977.

⁴S. Levit, Phys. Rev. C **21**, 1594 (1980).

⁵S. Levit, J. W. Negele, and Z. Paltiel, Phys. Rev. C **21**, 1603 (1980).

⁶S. Levit, J. W. Negele, and Z. Paltiel, *Proceedings of the Workshop on the Time Dependent Hartree Fock Method*, edited by Bonche et al. (Saclay, 1979).

⁷R. Feynman and A. R. Hibbs, *Quantum Mechanics and Path Integrals* (McGraw-Hill, New York, 1965).

⁸R. Balian, G. Parisi, and A. Voros, Phys. Rev. Lett. **41**,

1141 (1978).

⁹S. Coleman, Phys. Rev. D **15**, 2929 (1977); C. Callan and S. Coleman, *ibid.*, 1762 (1977).

¹⁰M. Gutzwiller, J. Math. Phys. **8**, 1979 (1967).

¹¹J. P. Blaizot and H. Orland, Saclay Report No. DPh-T/79-168.

¹²T. H. R. Skyrme, Philos. Mag. **1**, 1043 (1956).

D. Vautherin and D. M. Brink, Phys. Rev. C **5**, 626 (1972).

¹³P. Bonche, S. E. Koonin, and J. W. Negele, Phys. Rev. C **13**, 1226 (1976).

¹⁴J. W. Negele, S. E. Koonin, P. Möller, J. R. Nix, and A. J. Sierk, Phys. Rev. C **17**, 1098 (1978).

¹⁵J. W. Negele (unpublished).

¹⁶R. Balian and C. Bloch, Ann. Phys. (N.Y.) **85**, 415 (1974).

¹⁷This interpretation was suggested by A. K. Kerman.